

A deterministic approach to active debris removal target selection

Aleksander Lidtke

Astronautics Research Group, University of Southampton, UK

Hugh G. Lewis

Astronautics Research Group, University of Southampton, UK

Roberto Armellin

Astronautics Research Group, University of Southampton, UK

ABSTRACT

Many decisions, with widespread economic, political and legal consequences, are being considered based on the concerns about the sustainability of spaceflight and space debris simulations that show that Active Debris Removal (ADR) may be necessary.

The debris environment predictions are affected by many sources of error, including low-accuracy ephemerides and propagators. This, together with the inherent unpredictability of e.g. solar activity or debris attitude, raises doubts about the ADR target-lists that are produced. Target selection is considered highly important, as removal of non-relevant objects will unnecessarily increase the overall mission cost [1].

One of the primary factors that should be used in ADR target selection is the accumulated collision probability of every object [2]. To this end, a conjunction detection algorithm, based on the “smart sieve” method, has been developed and utilised with an example snapshot of the public two-line element catalogue. Another algorithm was then applied to the identified conjunctions to estimate the maximum and true probabilities of collisions taking place.

Two target-lists were produced based on the ranking of the objects according to the probability they will take part in any collision over the simulated time window. These probabilities were computed using the maximum probability approach, which is time-invariant, and estimates of the true collision probability that were computed with covariance information.

The top-priority targets are compared, and the impacts of the data accuracy and its decay highlighted. General conclusions regarding the importance of Space Surveillance and Tracking for the purpose of ADR are drawn and a deterministic method for ADR target selection, which could reduce the number of ADR missions to be performed, is proposed.

1. INTRODUCTION

It is a common belief that removing a number of uncontrolled objects from Earth orbit is necessary to halt the increase of the total number of objects, most of which are expected to be fragments resulting from collisions [3]. This phenomenon was indeed predicted before [4] but a lot more attention has been paid to it recently as the self-reinforcing effect of collisions generating more debris and thus more collisions has been stipulated to be inevitable even if no future launches took place [5]. This has sparked world-wide interest in the development of technologies to remove objects from the orbit and thus stopping the collision cascade.

Taking action in space debris remediation obviously implies the need to select the objects that should be removed. Due to the novelty of the technologies required to perform such removal missions, the cost of every such undertaking is expected to be high. Thus reducing the number of removal missions by selecting the targets more appropriately becomes important.

A common option for the selection of removal targets appears to be ranking all the objects based on 200 year-long Monte Carlo simulations and removing the ones that have the highest chance to be involved in collisions (collision probability) and collisions of which will have the highest severity (roughly proportional to mass) [2]. Given sufficient Monte Carlo runs, reliable statistics can be accumulated and the objects that are statistically the most likely to be involved in a collision can be identified. This leads to approximately 20 objects [2] that need to be removed to prevent a single collision thus increasing the capital cost of successful Active Debris Removal (ADR) even further.

These targets are not necessarily the ones that *will take part* in dangerous conjunctions, however, but rather the ones that are the *most likely to have* such conjunctions and thus be involved in a collision in the long-term. If the very hazardous conjunctions can be predicted more accurately and addressed at short notice the number of ADR missions may be reduced significantly. Furthermore, the decision to remove a given object could potentially be done based on accurate ephemerides and propagators rather than the current debris environment models that are considerably uncertain (population size can vary by as much as an order of magnitude [6]). This could remove part of the sources of errors in target selection.

Finally, the confidence in the space debris environment models and thus also the target lists being generated currently cannot be reliably quantified. The investments that may need to be made to make ADR successful are expected to be huge, and committing to such expenses with no confidence as to the outcome is unjustified.

Previous studies with DAMAGE, the evolutionary debris model of the University of Southampton, have hinted at the importance of individual conjunctions in the scope of the evolution of the entire debris population. The nature of the debris environment was therefore investigated in fine spatial and temporal resolutions to visualise the importance of such events that cannot be reliably captured and reflected in the target lists using the current models.

In order to achieve this, a completely new simulation framework that uses an adaptation of the algorithms used to identify conjunctions for spacecraft operation purposes was developed. This framework uses the simplified general perturbations (SGP4) propagator together with Two-Line Elements (TLEs) [7] as a proxy of orbital mechanics. This propagator is inaccurate when predictions are made for more than several days but it allows most of the major perturbing forces on a satellite to be modelled while being computationally fast, thus allowing large-scale debris environment simulations to be performed. The TLE uncertainty estimation methods that need to be used provide only approximate accuracy of the orbital elements, not the actual covariances. But these inaccurate ephemerides and estimated covariances suffice to identify the trends that are exhibited by the debris environment since the conjunctions need not be found accurately or collision probabilities estimated exactly to achieve this.

Description of the model developed, namely the algorithms used to detect conjunctions and calculate the collision probabilities, is given first. Then the study of the debris environment that has been performed is described and the results presented. Lastly, conclusions regarding the variability and unpredictability of the important conjunctions are made and an alternative approach to ADR target selection, based on “just-in time collision avoidance” [8], suggested.

2. METHODOLOGY

This section describes the methods that have been used to quantify collision probabilities of all the objects from the public Two-Line Element catalogue. These can, in principle, be estimated by looking at spatial densities of all the objects in various orbital regimes rather than conjunctions between individual objects [9]. This work will show, however, that it is the individual conjunctions that govern the behaviour of the entire space debris population and hence a set of algorithms that enables them to be resolved was needed.

2.1 Conjunction Detection

A conjunction has been defined as a time interval when two objects’ centres of mass are within a certain distance threshold from one another. Ellipsoidal threat volumes can also be used for conjunction screenings in order to tackle the position uncertainties that are not the same in every direction, but it was decided to account for this when computing the collision probability for every conjunction [10; 11]. Furthermore, conjunctions between more than two objects have been treated as multiple conjunctions between pairs of objects.

Even with such a simple formulation of a conjunction the computational time required to identify them between all the objects in the public catalogue (approx. 15 000 objects [12]) is significant. This raises the need to implement a number of so-called pre-filters that discard pairs of objects that cannot have a conjunction based on simple and fast to evaluate flight dynamics principles.

The entire simulation period was split into time intervals in which all the object pair combinations were analysed. The Cartesian position, velocity, and orbital elements of the objects at the beginning of every analysis interval were used to pre-filter the objects. If all the pre-filters were passed the minimum distance between the objects in this analysis interval would be found together with the corresponding time of closest approach (TCA). If the objects got closer than the threshold distance the collision probabilities would be computed and the conjunction recorded. The entire process was repeated in the following intervals until the end of the simulation was reached.

2.1.1 Pre-filtering Stage

A number of pre-filters have been developed to date, starting with the method by [13] that is still being used as well as alternative approaches adopted by [9], [14] and [15]. However, some pre-filters are not applicable to certain types of orbits (e.g. the orbit path filter that is only applicable to non-coplanar orbits [16]) or require the orbit to be provided in a specific format (e.g. mean elements [13]). Therefore, only the pre-filters that have been implemented to produce the results discussed herein, which are a modification of the “smart sieve” pre-filter set [15], will be presented for brevity. The filters will be described in the same order as they are implemented in the simulation code.

Every object in orbit can be associated with an altitude band where it resides, even if it does not follow an orbit that can be approximated as Keplerian. This forms the foundation on which the first pre-filter, the perigee-apogee filter, works [13]. Because of its generality and the fact that it does not produce false negatives [15] the perigee-apogee filter has been implemented in this work but with a contingency of 50 km. This is to say that the difference

between the perigee and apogee altitudes of the two objects at every analysis time step would need to be higher than the conjunction threshold distance plus 50 km in order for the pair not to be further analysed in the time interval. However, if the difference were 1000 km or more the pair would be discarded from further analysis in all the remaining intervals as the two objects would clearly not cross each other's altitude bands unless manoeuvres were performed and these have been ignored in this study. This was not implemented in the original "smart sieve" [15].

Another pre-filter, the X, Y, Z sieve, which makes no assumptions as to the trajectories of the objects of interest, was developed by [14] and also implemented by [15]. The sieve is only concerned with the components of the Cartesian positions of the objects at any given time. This filter uses an observation that if any Cartesian coordinate pair of two objects at the beginning of a given analysis interval varies by more than a certain screening threshold, c , here adopted from the "smart sieve", there is no chance that they could have a conjunction. For example, a potential conjunction pair, i and j , will be rejected using the z coordinate if

$$|z_i - z_j| > c. \quad (1)$$

Limiting the problem to Earth-satellites allows further simplifications, firstly by observing that no objects can move with respect to each other faster than twice the surface escape velocity at any time [15]. If the analysis interval is known, a distance, R_{th} , referred to as the threshold radius in [15], may be defined:

$$R_{th} = R_{conjunction} + v_{escape} \times \Delta T. \quad (2)$$

If the distance between the two objects at the beginning of the analysis time step, ΔT , is greater than this threshold value the two objects cannot get within the conjunction distance threshold, $R_{conjunction}$, during this analysis interval [15]. Furthermore, if a given object pair is separated by more than R_{th} at the beginning of the given time interval, a number of subsequent intervals may be skipped [15] as

$$N_{skip} = int\left(\frac{r - R_{th}}{2}\right), \quad (3)$$

where r is the actual separation distance between the objects at the beginning of the analysis time step, and int denotes the integer part of a number.

Equation (2) does not account for the effects of gravity, i.e. it assumes linear relative motion. The maximum acceleration between a pair of objects can never exceed twice the surface value, g_0 [15]. Hence, a maximum distance, R_{acc} , can be established that ensures that the secondary object, if it does get within $R_{conjunction}$ from the primary in the current time step, will be picked up in the same fashion as with the threshold radius but accounting for the acceleration effects:

$$R_{acc} = R_{conjunction} + g_0 \times \Delta T^2. \quad (4)$$

All the above pre-filters have been adopted from [15] but during testing it was discovered that the "smart sieve" steps that use the threshold radius given in equation (2) occasionally produced false negatives. However, when a contingency factor of 2.0 was used, i.e. when twice the threshold radius was used instead, no false negatives were present for all the tested orbital regimes. This was the only additional change that has been made to the "smart sieve".

2.1.1 Range-based Detection

If all the pre-filter stages are passed the time of the closest approach is computed by finding the epoch at which the relative range-rate is zero.

Even though a freeware implementation of the SGP4 propagator was used to generate the ephemerides for the study described herein [17] the simulation framework has been designed to accept any ephemerides sources. Being able to cope with externally-generated ephemeris tables was of primary importance as it allows high-fidelity propagators to be used with the same framework.

In order to keep the simulation framework insensitive to the ephemeris source an ephemeris table is generated using SGP4 and only the states propagated to the analysis interval epochs are used. These states are interpolated using a piecewise cubic polynomial expressed in a dimensionless time domain in order to avoid singularities. This ensures that the velocity and position are continuous between the neighbouring intervals and limits the number of floating point operations that need to be performed in order to generate the interpolating polynomials.

This interpolation scheme allows the relative range, range rate $v(t_k)$ and acceleration $a(t_k)$ between the two objects to be expressed analytically as 6th, 5th, and 4th order polynomials, respectively. This enables the epoch of the closest approach to be found using a simple Newton-Rhapson search [18] to find the point where the relative range rate (square of the range rate is used here to provide computational time saving) is zero. The Newton-Rhapson search is initialised in the middle of the interpolation interval and performed in the following manner [15]:

$$t_{+1} = t_k - \frac{v(t_k)}{a(t_k)}, \quad (5)$$

where k is the index of current iteration in finding the root of the relative range rate squared. The number of iterations is limited to 1000 and the TCA convergence to 10^{-8} of the time step (which corresponds to 6×10^{-6} seconds for the nominal time step duration of 600 seconds). The root finding is, as conventionally adopted, terminated when the desired accuracy is reached or when the maximum number of iterations has elapsed [18].

When the relative range rate is zero a check on the second derivative, i.e. the relative acceleration, should be performed to ensure that a minimum was found rather than a maximum. However, if a maximum were found the relative distance at the TCA would be greater than the conjunction threshold so a range, rather than a second derivative, check can be performed to verify what type of local extreme was found. Normally if roots of the relative range-rate are real, which they will be when using the numerical scheme described herein, they will correspond to minima of the relative range [10].

The analysis interval of 600 seconds was chosen as the computational speed of the entire framework was the greatest with such a step (it is expected for such algorithms to have an optimum time step [15]) and no very close conjunctions were missed. Specifically, the interpolation scheme was accurate to within 20 km (infinity-norm) for all the investigated orbit types. Hence, setting the conjunction threshold distance to 20 km guaranteed that no very close conjunctions, which could potentially have extremely high collision probabilities, would be missed. Note that SGP4 accuracy decay was not accounted for here as finding all the conjunctions that would occur in the real world was not the goal of this study.

2.2 Collision Probability Estimation

Computing the true collision probability for every conjunction requires the covariance of the ephemerides of both objects to be known and propagated to the TCA and the publically-available ephemerides' sources (TLEs) are not provided with covariances [12]. This is a major obstacle for virtually all researchers and spacecraft operators that do not have access to a catalogue of their own. This forces the operators to rely on conjunction summary messages published by the Joint Space Operations Center (JSpOC) and the researchers to rely on computing the collision probabilities using objects' spatial densities or other algorithms [19; 20; 21; 22].

An alternative solution to the issue of unavailable TLE covariance has been adopted in this work and will now be described. Then a set of algorithms that were used in order to compute the maximum and estimate the true collision probabilities from this covariance will be presented.

2.2.1 Public Catalogue Covariance Estimation and Propagation

Even though the covariances of the TLEs computed with respect to orbits propagated with high-fidelity numerical propagators [20; 23] should be used for operational purposes (making decisions about collision avoidance manoeuvres or dedicated tracking campaigns) this study was aimed at investigating trends in the space debris environment so alternatives were considered. Since the predictions were made using TLEs it was the internal variability and inconsistency of these element sets that was of interest rather than how the TLE-derived states relate to reality. This allowed the trends in the debris environment and our capability to predict those to be analysed.

A method to estimate the covariance of a TLE based on previous TLEs for the same object was developed by [24] and implemented in this work. All the historical TLEs spanning a period of 14 days from the epoch of the TLE used for conjunction detection were gathered and the residuals were computed w.r.t. that most-recent TLE for every object. The covariance matrix could then be computed according to the method given by [24]. If fewer than five TLEs were available for a given object it would be discarded from the analysis entirely as no covariance could be estimated with so few observations. Note that true covariance should be used if this ADR approach were followed.

Moreover, certain TLEs had to be ignored in case they were erroneous or a manoeuvre had been conducted by the spacecraft in the 14-day time window. In order to do this, specific orbital energies of all the TLEs from the two-week window were analysed and the TLEs whose energies were more than three standard deviations above the average were rejected [25].

Note that such derivation of the TLE covariance can readily be used to propagate the covariance to any epoch – it suffices to propagate all the TLEs for the given object to the specified epoch and re-compute the covariance. This allowed collision probability to be computed using this covariance at the TCA that reflects our capability to predict a given collision. Given the covariance estimation method this cannot be referred to as the actual collision probability and its sole purpose is to visualise the evolution of the data accuracy with time. It will, however, be henceforth referred to as the “true” collision probability for brevity.

The covariance matrix can also be scaled to quantify the maximum collision probability during a given conjunction [26]. The maximum collision probability is largely time-invariant as it is not affected by the growth of the covariance and hence probability dilution. Indeed the probabilities of events occurring in reality are not a function of the time at which they are predicted and thus the maximum probability can be thought of as a means to highlight the events that would be likely to result in a collision in reality.

The maximum collision probability is found by scaling the previously estimated covariance matrix (denoted as C) by a scaling factor, k . The latter can be found analytically by assuming that the probability takes its peak value when the relative position's probability density function (PDF) does (as given in e.g. [26]):

$$k = \sqrt{\frac{p_{mean}^T C^{-1} p_{mean}}{2}}, \quad (6)$$

where p_{mean} is the mean relative position vector of the two objects at the conjunction epoch. This analytical estimate has been found not to be accurate for all conjunctions. Therefore a simple golden-ratio search was utilised to find the scaling factor k that yields the actual maximum of the collision probability of every conjunction [18].

Computing both the "true" and maximum probabilities also allowed the collision probabilities that are truly exhibited in the debris environment to be approximated – the maximum collision probability estimates the upper bound while the "true" collision probability computed using the estimated TLE covariance the lower bound. This is because the larger the covariance the lower the collision probability (a phenomenon commonly referred to as probability dilution) and the chosen covariance estimation method produces larger uncertainties than what is believed to be the actual TLE covariance computed by comparison to high-fidelity numerical propagators [23; 27].

2.2.2 Collision Probability Estimation

A classical approach, where every conjunction is analysed in a B-plane frame of reference centred on the primary (arbitrarily chosen because both objects are equally important in this study) was adopted [26; 28; 29].

The position covariances of both objects are propagated to the TCA, rotated to the B-plane according to the algorithm given e.g. by [26], and combined. The velocity covariance is ignored as it has been found not to affect the collision probability significantly [26] and this has been confirmed by Monte Carlo analyses of several exemplar conjunctions. Collinear relative motion is assumed in the vicinity of the TCA thus allowing the covariance matrix to be projected onto the B-plane and reducing the number of dimensions of the problem from three to two [26; 29].

The position covariance matrices are then converted into a probability density function and numerically integrated in the Cartesian coordinates in the B-plane (y, z) inside a circle with radius equal to the combined radii of the two objects (collision radius r) and centred on the primary as given in [26; 29]:

$$P = \iint_{\substack{z=r; y=\sqrt{r^2+x^2} \\ z=-r; -y=\sqrt{r^2+x^2}}} \frac{2\pi}{\sqrt{\det(C)}} e^{-\frac{1}{2}D^T C^{-1} D} dy dz. \quad (7)$$

In the above equation det denotes the determinant of the matrix and D is the discrepancy vector defined as:

$$D = \begin{bmatrix} y \\ z \end{bmatrix} - p_{mean}, \quad (8)$$

where y and z are instantaneous values of the free Cartesian in-plane. Even though equation (7) can be expressed as an infinite series of analytical terms, thus reducing the time required to compute the collision probability of every conjunction [29], this approach has been found to be inaccurate in some cases and thus a simple numerical integration scheme [18] was used instead.

Integrating equation (7) yields the probability that both objects' centres of mass will be within the collision radius during the closest approach, i.e. whether a collision will take place. The maximum collision probability can be computed in the same manner as well if the covariance matrix is scaled beforehand, as mentioned previously.

TLEs come with no information as to the size of the associated objects and thus certain assumptions had to be made in order to enable the collision probability to be computed. These will be described in the following section.

2.2.3 Physical Object Size

A database containing the physical radii of objects launched up to 2003 (up to NORAD catalogue number 28057) originally compiled by The Aerospace Corporation was kindly provided by T.S. Kelso, thus allowing the collision radius to be computed as accurately as possible for some conjunctions. This implies ignoring the attitude of the objects but this is not expected to change the global trends in collision probabilities as it would only affect the relative importance of individual conjunctions. Such a simplification is therefore perfectly acceptable for this study but should be addressed if an *ad hoc* collision prevention is to be implemented.

For the remainder of the catalogue, the MASTER 2009 population, kindly provided by the ESA Space Debris Office, was analysed and the size of the objects with respect to their type was investigated. An average radius for rocket bodies (R/B), payloads (P/L), mission-related objects (MRO), and debris (DEB) was computed. The standard deviation of every group was also found and the results are shown in Table 1.

Some of the MASTER object types can be directly linked to TLEs through the three-line elements that contain information about the type of certain objects. As the three-line element catalogue does not distinguish mission-

related objects, the data for this type of object were not directly utilised. Moreover, the three-line element database contains many objects that are not classified as payloads, rocket bodies or debris. For these objects the average size of the entire MASTER 2009 (all four types of objects) population was used.

Table 1: ESA’s MASTER 2009 population objects’ radii grouped according to the types of objects (rocket bodies (R/B), payloads (P/L), mission-related objects (MRO), and debris (DEB)) also discerned in Space-Track’s Three-Line Elements.

Object type	R/B	P/L	MRO	DEB	Other
MASTER Object ID	1	2	3	4	1, 2, 3, and 4
Average radius (m)	1.7691	1.7691	0.5385	0.1558	0.3470
Standard deviation (m)	0.8145	0.7824	0.7219	0.5545	0.7803

It was decided that, in the absence of an exhaustive database of object sizes that could associate every Space Surveillance Catalog number (SSC) with a particular object size the statistical values from Table 1 should be assumed whenever an object’s size was not available in the database. Even though the standard deviation for certain types of objects is large it has been found not to affect the overall collision probability by more than approximately 10% when an average MASTER 2009 radius \pm one standard deviation is used as long as a database of the object sizes is utilised for the remaining objects.

3. RESULTS

A set of TLEs from the 23rd October 2013 was used to find all the conjunctions between all the objects in the public catalogue over 30 days. Only the objects for which enough historical TLEs were available to estimate the TLE covariance (11680 out of 14917 objects) were used. As mentioned previously, conjunctions closer than 20 km (3 123 779 in total) were identified and collision probabilities computed for those.

For every object the probability of collision with any other object over the entire simulation was computed. The entire set of objects was then ranked based on these accumulated “true” and maximum collision probabilities.

Compiling the list using the “true” collision probability allowed the impact of the deteriorating orbit prediction to be visualised. The maximum probability list, on the other hand, was more representative of the actual behaviour of the debris environment – even though the maximum probabilities tend to be several times higher than the actual ones, the probability of an event occurring in reality does not depend on how much in advance the given event is forecast. In other words it is only our ability to predict events that depends on the prediction period, not the probability of the events themselves, and it was the order of the objects in the target list rather than value of the collision probability that was of the most interest.

The evolutions of the accumulated collision probabilities for the ten top objects in either list are presented in Fig 1 and Fig 2 for the “true” and maximum probability target rankings, respectively. The corresponding lists of targets, together with the final collision probabilities accumulated after the one month-long simulation and the highest collision probability of a single conjunction recorded, are summarised in Table 2.

Firstly, it can be noted when examining Fig 2 that it was merely several conjunctions out of over 3.1 million that defined the objects with the highest overall maximum collision probability. This agreed with DAMAGE simulations where such behaviour had also been observed. In fact, the highest maximum collision probability event contributed 98.8% to the final accumulated collision probability of Meteor 2-3. Upon examination of the top objects from the maximum probability-based target list one will notice that such behaviour, where individual conjunctions dictated the macroscopic behaviour of a given object, was exhibited by six of the top ten targets. Large contributions of individual conjunctions with extremely high maximum probabilities, albeit with less impact on the total accumulated probability, can be observed in cases of most of the other objects as well.

What is more, even the order of the top-six object was defined by those three conjunctions involving METEOR 2-3 and FENGYUN 1C DEB, GEOSAT and COSMOS 2251 DEB, as well as SL-16 R/B and COSMOS 2251 DEB. This means that not only the behaviour of the probability of individual objects but the entire environment (the objects with the highest maximum collision probability over a month) has been established by only three events.

The behaviour of the objects from the “true” probability list was completely different, however – the individual conjunctions typically contributed at most a few percent to the overall accumulated collision probability. This was only different for the conjunction of Envisat and Pegasus R/B – this event contributed 29.4% and 97.1% to the final accumulated “true” collision probabilities of both objects, respectively. This was only because this event occurred on 24 Oct 2013 11:18.25 i.e. merely 31.3 and 47.1 hours after the epochs of the TLEs used to find conjunctions for Envisat and Pegasus R/B, respectively. These short prediction periods meant that the covariances for these objects had not grown sufficiently to dilute the collision probability of this conjunction.

Only one object from the maximum probability list in Table 2 is present on the “true” probability list as well. Its position in the ranking is vastly different, however.

165 objects decayed during the duration of the simulation according to [12]. All the conjunctions involving these objects after their decay epoch were excluded from the results. Unfortunately [12] provides only approximate decay epochs (accurate to within one day), therefore certain conjunction could have been erroneously filtered out. Determining the re-entry epoch more accurately using the SGP4 propagator was attempted but it was realised that it did not model objects’ trajectories accurately close to re-entry and returned erroneous state vectors (orbital velocities in the order of cm sec^{-1}). Hence, this was not investigated any further in the absence of data and tools.

Table 2: Two target lists based on accumulated “true” and maximum collision probabilities after one month. Highest collision probability of individual conjunctions for every object is also given.

Priority	"TRUE" PROBABILITY-BASED				MAXIMUM PROBABILITY-BASED			
	SSC	Name	Final P_C	Highest Individual P_C	SSC	Name	Final P_C	Highest Individual P_C
1	27386	ENVISAT	9.1E-06	2.7E-06	10514	METEOR 2-3	5.8E-02	5.8E-02
2	25171	IRIDIUM 54	4.9E-06	9.4E-08	31214	FENGYUN 1C DEB	5.8E-02	5.8E-02
3	10514	METEOR 2-3	4.8E-06	2.3E-07	15595	GEOSAT	8.5E-03	8.0E-03
4	39087	AAUSAT3	3.6E-06	3.8E-08	35836	COSMOS 2251 DEB	8.0E-03	8.0E-03
5	28057	CBERS 2	3.3E-06	1.7E-07	25400	SL-16 R/B	6.5E-03	6.3E-03
6	27450	IRIDIUM 97	3.0E-06	4.2E-08	33812	COSMOS 2251 DEB	6.3E-03	6.3E-03
7	23106	PEGASUS R/B	2.8E-06	2.7E-06	17369	COSMOS 1818	3.2E-03	2.5E-04
8	14452	METEOR 2-10	2.3E-06	1.1E-07	22830	ARIANE 40 R/B	3.1E-03	2.4E-03
9	24971	IRS 1D	2.1E-06	9.4E-08	18187	COSMOS 1867	3.0E-03	2.9E-04
10	34071	IRIDIUM 33 DEB	2.0E-06	4.4E-07	27386	ENVISAT	2.9E-03	5.6E-04

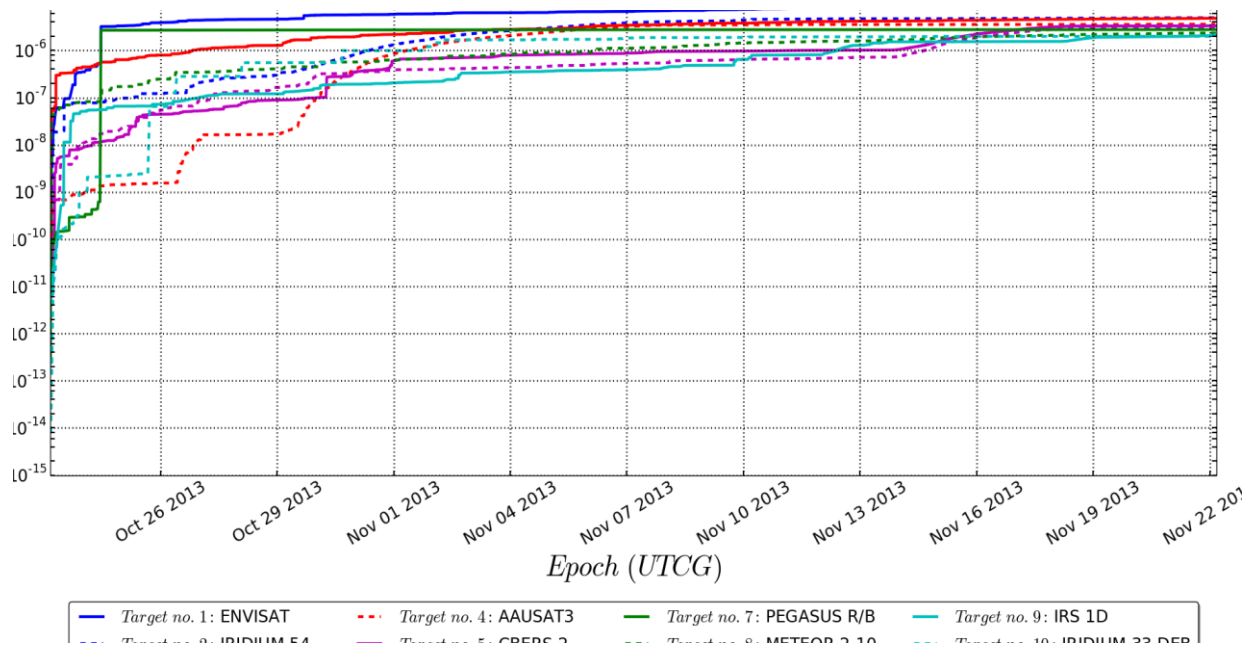


Fig 1: History of the accumulated “true” collision probability (probability of any of the previous collisions taking place) as a function of epoch for ten objects with the highest “true” collision probability after one month.

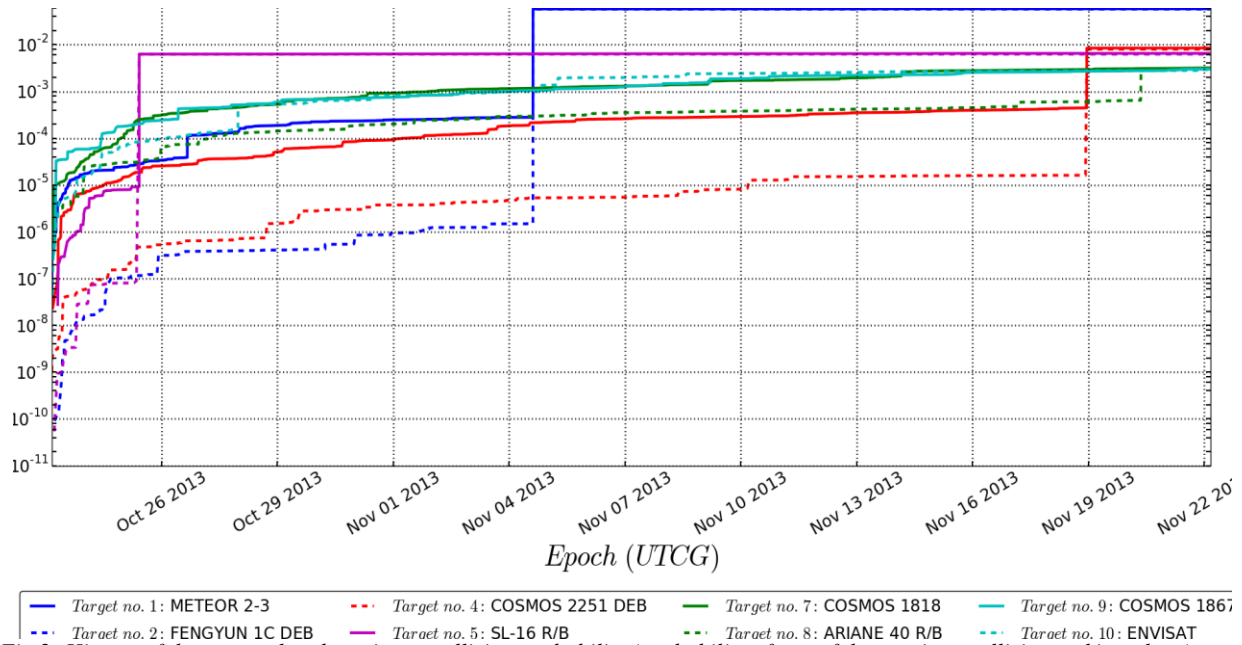


Fig 2: History of the accumulated maximum collision probability (probability of any of the previous collisions taking place) as a function of epoch for ten objects with the highest maximum collision probability after one month.

4. DISCUSSION

It has been pointed out that the collision probability of individual events that can be predicted decreases the more distant in time the prediction. This is indeed expected as the covariance grows in time thus leading to the probability of even the same conjunctions (identical object sizes and conjunction geometries) to decrease. This is a mathematical representation of the simple and trivial fact that the further ahead one tries to predict something the less certain the prediction is.

One can notice that the composition of the “true” probability target list does not change approximately three weeks after the beginning of the simulated time window. All significant changes in the absolute value of the “true” collision probability, however, take place in the first seven days of the simulation. The most dramatic events, i.e. conjunctions with the highest individual collision probabilities, can only be predicted in the first few days or even hours. Beyond approximately 26 Oct 2013 only one conjunction with relatively large change (36.8%) in the collision probability was recorded for the top ten objects (involving CBERS 2 on the 30 Oct 2013).

The maximum collision probability is independent of time and very dangerous, in terms of collision probability, events can occur at any instance. This is indeed what one would expect to take place in real life and this is why this part of the simulation may be referred to as a “proxy of reality”.

The fact that only one object from the maximum probability list was found on the “true” probabilities list is perhaps the most profound yet the least surprising finding of this study. Namely, given quickly deteriorating orbital information, we cannot confidently predict all the most important conjunctions far in advance and this finds its reflection in the ADR target lists.

Based on the results of this study it is impossible to judge the actual limits of our ability to predict orbital collisions, but these results suffice to visualise the impact of the deteriorating data accuracy on the target lists. However, even if the highest-accuracy data and propagators are used, it is not expected that the prediction could be made for more than several days [30] for a given collision probability threshold to be exceeded. Computing the maximum collision probability for all the conjunctions and basing the preliminary decision thresholds on this metric could potentially extend this period significantly. But the final decision should not be based on this metric as it is artificial and does not reflect our confidence in the prognoses.

Clearly, an architecture that would need to be put in place to be able to prevent collisions with little advance warning would differ significantly from the currently envisioned ADR ideas, many of which are being optimised to remove as many objects in one year as possible [1; 31]. Perhaps it would not even need to be space-borne or require physical contact to be made with an uncooperative target. Certainly the longer the collision advance warning period the easier it would be to implement a mission to prevent it. This can only be achieved if improvements in the Space Surveillance and Tracking (SST) systems as well as propagators and force models are made. Still, extremely rapid deployments (lead times in the order of days) seem inevitable.

Depending on how accurate collision prediction is the prevention risk threshold may be set higher. This will reduce the cost of such an approach to ADR but will increase the ignored collision risk, thus making it more likely that a collision will take place despite the efforts to prevent collisions from occurring. This is a very important trade off that will affect the cost of such an ADR architecture as well as its return and a further study addressing this issue is envisioned. If the action risk threshold is set too low, an *ad hoc* collision prevention may not offer any cost savings compared with the traditional ADR concepts as more conjunctions will need to be addressed. An irrefutable merit of this approach c.f. removing statistically important objects is the capability to set the accepted risk threshold at the expense of preventing more collisions, however.

5. CONCLUSIONS

Firstly, the importance of individual conjunctions in terms of the collision probability of individual events has been highlighted. This has been derived using ephemerides and algorithms completely different from those currently used in the evolutionary debris models but the same conclusion about the importance of individual conjunctions can be drawn from both. This increases the confidence in the trends that have been identified as they do not appear to change regardless of the fidelity of the simulations and algorithms.

The ability to predict the important conjunctions has also been investigated. The rapid decrease of the prediction confidence has been highlighted and the feasibility to implement a responsive Active Debris Removal system that would remove objects from orbit after identification of a potential collision has been questioned. A study using different ephemeris and covariances sources would need to be conducted in order to fully address its feasibility.

It is still likely that any system that relied on the most-recent ephemerides and extremely short-term predictions would be able to, at most, apply sufficient ΔV to either object to prevent a collision from taking place. Another potential way to exploit the ADR framework presented herein would be to further develop space systems allowing very rapid deployments and adapt them to perform ADR [32].

What follows is that the areas of technology that require development to implement an *ad hoc* collision prevention approach or a more classical ADR architecture differ significantly. They also have different synergies, i.e. would contribute towards development of technologies useful in different applications. As already mentioned, the “just in time collision avoidance” requires capable Space Surveillance and Tracking, potentially also very rapid access to space with extremely short lead times. Developments in these areas may be of more interest to the decision makers than advanced guidance, navigation and control as well as technologies needed to rendezvous and dock with an unprepared, uncooperative target.

It is recommended that a discussion about the fundamental approach to Active Debris Removal should be initiated amongst the decision makers and the benefits of *ad hoc* collision avoidance should be thoroughly evaluated. This is primarily because such an approach may not only prevent more orbital collisions than other ADR architectures but also potentially provide cost savings due to fewer missions that may need to be flown. If individual ADR missions pose a significant collision threat, being able to fly fewer of them would also reduce the risk of causing a collision while trying to remove objects from orbit.

Furthermore, unlike the stochastic target selection schemes, targeting the likely collisions would enable the collision prevention probability threshold to be set. This would enable the residual risk due to the conjunctions being ignored to be quantified and traded off against the cost of preventing more collisions. Of course nothing can ever be predicted with absolute certainty and any approach to ADR target selection will still be probabilistic, unless all the uncontrolled objects are removed. However, having confidence in the results of ADR and being able to control the residual risk can never be realised with any other target selection schemes.

6. ACKNOWLEDGEMENTS

The authors would like to thank the ESA Space Debris office for allowing them to use the MASTER 2009 population. Dedicated thanks go to Dr Holger Krag and Dr Tim Flohrer for their extremely valuable feedback and help in validating the collision probability algorithms.

Big thanks to Dr David Vallado for distribution of the SGP4 propagator code, without which this research would never be possible in the timeframe available.

The authors would also like to express their gratitude to Dr T.S. Kelso for useful comments regarding the collision probability, maintaining the CelesTrak website and provision of the objects’ physical radii database.

The authors would also like to acknowledge the use of AGI’s Systems Toolkit in the verification process of the developed simulation framework.

7. REFERENCES

1. Pasa, N. et al, *Target selection and comparison of mission design for space debris removal by DLR’s advanced study group*. September–October 2014, s.l.: Acta Astronautica, 2014, Vol. 102. ISSN 0094-5765.

2. Liou, J.C. *An active debris removal parametric study for LEO environment remediation*. s.l.: Advances in Space Research, 2011, Vol. 47.
3. Liou, J.C. *Collision activities in the future orbital debris environment*. 9, s.l.: Advances in Space Research, 2006, Vol. 38.
4. Kessler, D. J., B.G. Cour-Palais. *Collision frequency of artificial satellites - The creation of a debris belt*. s.l.: Journal of Geophysical Research, 1978, Vol. 83.
5. Liou, J.C., N.L. Johnson. *Instability of the present LEO satellite populations*. s.l.: Advances in Space Research, 2008, Vol. 41.
6. White, A.E., H.G. Lewis. *The many futures of active debris removal*. s.l.: Acta Astronautica, 2014, Vol. 95.
7. Hoots, F.R., R.L. Roehrich. *SPACETRACK REPORT NO. 3 Models for Propagation of NORAD Element Sets*. s.l.: United States Department of Defense, 1988.
8. McKnight, D. *System Engineering Analysis of Derelict Collision Prevention Options*. Naples, Italy: 63rd International Astronautical Congress, 2012.
9. Khutorovsky, Z.N. et al, *Direct method for the analysis of collision probability of artificial space objects in LEO: techniques, results and applications*. Darmstadt, Germany: s.n., 1993. First European Conference on Space Debris.
10. Alfano, S. *Determining Satellite Close Approaches, Part II*. 2, 1994, The Journal of Astronautical Sciences, Vol. 42, pp. 143-152.
11. Coppola, V. Woodburn, J. *Determination of Close Approaches Based on Ellipsoidal Threat Volumes*. 1999, Advances in Astronautical Sciences, Vol. 102, pp. 1013-1024.
12. JFCC SPACE/J3. Space-Track. [Online] Scitor. [Cited: 11 August 2014.] <https://www.space-track.org>.
13. Hoots, F.R., L.L. Crawford, R.L. Roehrich. *An Analytic Method to Determine Future Close Approaches*. 1984, Celestial Mechanics, Vol. 33, pp. 143-158.
14. Healy, L.M. *Close Conjunction Detection on Parallel Computer*. 4, 1995, Journal of Guidance, Control, and Dynamics, Vol. 18, pp. 824-829.
15. Rodriguez, J.R.A., Fadrique, F.M.M., Klinkrad, H. *Collision risk assessment with a 'smart sieve' method*. Noordwijk, the Netherlands: s.n., 2002. Joint ESA-NASA Space-Flight Safety Conference.
16. Woodburn, J., V. Coppola, F. Stoner. *A description of filters for minimizing the time required for orbital conjunction computation*. Pittsburgh: s.n., 2009. AAS-AIAA Astrodynamics Specialist Conference.
17. Kelso, T.S. Satellite Tracking Software. [Online] Celestrak, 22 Jan 2000. [Cited: 26 Apr 2014.] <http://www.celestrak.com/software/tskelso-sw.asp>.
18. Press, W.H et al, *Numerical Recipes in C++, Second Edition*. Cambridge, UK: Cambridge University Press, 2002.
19. Flohrer, T. et al, *Operational Collision Avoidance for LEO Satellites at ESA*. Okinawa, Japan : s.n., 2011. Proceedings of the 28th International Symposium on Space Technology and Science (ISTS).
20. Floherer, T., H. Krag, H. Klinkrad. *ESA's process for the identification and assessment of high-risk conjunction events*. 44, 2009, Advances in Space Research, pp. 355-363.
21. Dominguez-Gonzalez, R., N. Sanchez-Ortiz. *Classification of TLE-catalogue objects in regard to their long-term collision probabilities*. Paris, France: 3rd European Workshop of Space Debris Modelling and Remediation, CNES, 2014.
22. Kessler, D.J. 1, s.l.: Icarus, 1981, Vol. 48.
23. Flohrer, T. *Personal communication*. 3 June 2014.
24. Osweiler, V. P. *Covariance estimation and autocorrelation of NORAD two-line element sets*. Wright-Patterson Air Force Base, OH, USA: Air Force Institute of Technology, 2009.
25. Patera, R.P. *Space Event Detection Method*. 3, 2008, Journal of Spacecraft and Rockets, Vol. 45, pp. 554-559.
26. Berend, N. *Estimation of the probability of collision between two catalogued orbiting objects*. 1, 1999, Advances in Space Research, Vol. 23, pp. 243-247.
27. Flohrer, T. et al, *Assessment and Categorization of TLE Orbit Errors for the US SSN Catalogue*. Wailea, HI, USA: s.n., 2008. Proceedings of the Advanced Maui Optical and Space Surveillance Technologies Conference.
28. Alfano, S. *Review of Conjunction Probability Methods for Short-term Encounters*. Colorado Springs, CO, USA: American Institute of Aeronautics and Astronautics, 2006.
29. Chan, K. *International Space Station Collision Probability*. Chantilly, VA, USA: The Aerospace Corporation, 2009.
30. Krag, H. *Personal communication*. Paris, France, 14 June 2014.
31. Cerf, M. *Multiple space debris collecting mission – debris selection and trajectory optimization*. s.l.: Journal of Optimization Theory and Applications, 2013, Vol. 156.
32. *ORS Operationally Responsive Space*. [Online] [Cited: 1 September 2014.] <http://ors.csd.disa.mil/>.